Draft version February 10, 2022
Typeset using LaTeX default style in AASTeX631

Magnetic Switchback Occurrence Rates in the Inner Heliosphere: Parker Solar Probe and 1 au

Francesco Pecora,[1] William H. Matthaeus,[1] Leonardo Primavera,[2] Antonella Greco,[2] Rohit Chhiber,[1,3] Riddhi Bandyopadhyay,[4] and Sergio Servidio[2]

[1] *Department of Physics and Astronomy, University of Delaware Newark, DE 19716, USA*
[2] *Dipartimento di Fisica, Università della Calabria 87036 Arcavacata di Rende, Italia*
[3] *Heliophysics Science Division, NASA Goddard Space Flight Center Greenbelt, MD 20771, USA*
[4] *Department of Astrophysical Sciences, Princeton University Princeton, NJ 08544, USA*

ABSTRACT

The subject of switchbacks, defined either as large angular deflections or polarity reversals of the magnetic field, has generated substantial interest in the space physics community since the launch of Parker Solar Probe (PSP) in 2018. Previous studies have characterized switchbacks in several different ways, and have been restricted to data available from the first few orbits. Here, we analyze the frequency of occurrence of switchbacks per unit distance for the first full eight orbits of PSP. In this work, are considered switchback only the events that reverse the sign of magnetic field relative to a regional average. A significant finding is that the rate of occurrence falls off sharply approaching the sun near 0.2 au (40 $R_\odot$), and rises gently from 0.2 au outward. The analysis is varied for different magnetic field cadences and for different local averages of the ambient field, confirming the robustness of the results. We discuss implications for the mechanisms of switchback generation. A publicly available database has been created with the identified reversals.

Keywords: Suggested keywords

1. INTRODUCTION

The orbit of Parker Solar Probe (PSP) has taken the mission into previously unexplored regions of the heliosphere in which both new phenomena, related to the origin of the solar wind, and known ones, from a rather different perspective, can be observed (Fox et al. 2016). The phenomenon of magnetic field "switchbacks" (SBs), defined either as large deflections, or polarity reversals relative to ambient conditions, has been previously observed at larger distances (Borovsky 2016; Horbury et al. 2018), but it is more evident in the PSP environment close to the sun.

A number of studies prior to PSP had already noted the existence of switchbacks in the interplanetary magnetic field (McCracken & Ness 1966; Neugebauer & Goldstein 2013; Borovsky 2016; Horbury et al. 2018). The origin of these switchbacks or "folds" has usually been discussed in association with phenomena closer to the sun, such as interchange reconnection (Fisk & Kasper 2020; Schwadron & McComas 2021; Bale et al. 2021) or some form of local dynamical activity (e.g., Ruffolo et al. 2020; Squire et al. 2020). Generally, polarity reversals at the heliospheric current sheet have been treated as a separate class.

Recently, numerous studies have examined detailed properties of switchbacks in PSP data (Horbury et al. 2020; Laker, R. et al. 2021; Mozer et al. 2020; McManus et al. 2020; Mozer et al. 2021; Tenerani et al. 2021), while other studies have provided insight into both the possible origin of switchbacks (Landi et al. 2006) and their propagation and dissipation (Tenerani et al. 2020; Magyar et al. 2021a,b).

fpecora@udel.edu

The purpose here is to provide a more complete perspective of the occurrence rates of switchbacks by employing the data from the initial eight orbits of PSP in a unified analysis. For specificity, we will consider strong switchbacks that reverse the local polarity of the magnetic field, corresponding to deflection angles greater than 90°.

The paper is organized as follows: criteria for data selection and the definition of switchbacks are given in Sec. 2; The statistics of SB waiting times and duration is presented in Sec. 3; The radial occurrence of SBs throughout the inner heliosphere is shown in Sec. 4; The last section is dedicated to the discussion of the results. Finally, in the appendix, the SB database is presented.

2. DATA SELECTION & SB IDENTIFICATION

We use publicly available measurements of magnetic field from the MAG instrument on the FIELDS (Bale et al. 2016), and solar wind ion speed from SPC on the SWEAP (Kasper et al. 2016) suites on the Parker Solar Probe (Fox et al. 2016) during its first 8 orbits. The analysis, from 2018 August 12 through 2021 June 19, is carried over non-overlapping 6-hour-long intervals as suggested in (Dudok de Wit et al. 2020; Bandyopadhyay, R. et al. 2021). The following procedure has been automatized using the python library AI.CDAS that provides access to CDAS database through CDAS REST API. The API service provided by CDAS is an advantageous tool that allows a user to request data from the server and work with them dynamically. A 6h interval is considered for the analysis only if, when divided in six 1h-long subintervals, each subinterval has less than $\sim$ 30 % missing points. In that case, linear interpolation is performed to restore data continuity (if any missing point is present). Intervals with more than $\sim$ 30 % missing points have been discarded. The same criterion has been used to skim Wind measurements, over the same period, for the magnetic field (MFI, Lepping et al. 1995) and bulk speed (SWE, Ogilvie et al. 1995)). The detection of SBs was carried out using magnetic field measurements at 10s and 60s resolutions. To ensure that the choice of the above settings does not affect the results, the analyses have been repeated changing the interval length to 3 hours, and choosing a more strict limit of 15% missing points per subinterval. We find a general consistency of results for the above variation of parameters. Therefore, the following analyses have utilized an interval duration of 6-hour and a $\sim$ 30% threshold in order to retain more intervals and a larger number of events.

The presence of switchbacks in each 6h interval, is revealed using the "normalized deflection" measure z as defined by Dudok de Wit et al. (2020)

$$z = \frac{1}{2}\left[1 - \cos(\alpha)\right], \tag{1}$$

where α is the angle between the pointwise magnetic field and a local average $\langle \mathbf{B} \rangle$ evaluated over the considered 6 hours. "Switchbacked" regions are those with a value of $z \geq 0.5$ corresponding to magnetic field deflections larger than 90° with respect to the local average. This is the main criterion employed in this study to define a switchback. This seems to us to be less arbitrary than a choice of other thresholds for z that indicate non-reversing deflections.

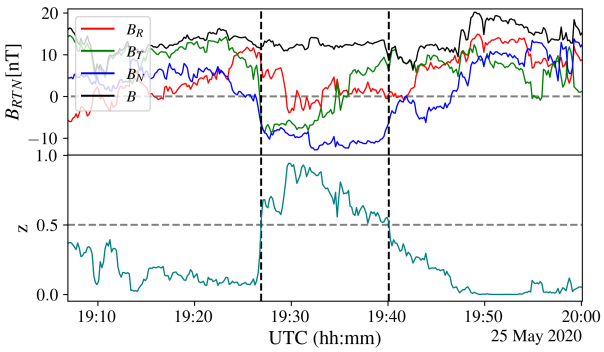

Figure 1. Example of a PSP time interval containing a switchback, as defined in Eq. 1 and by Dudok de Wit et al. (2020). (Top panel) magnetic field measurements at 10s resolution. (Bottom panel) The switchback, delimited by the two vertical dashed lines, is identified in the interval where $z \geq 0.5$, and extends for $\sim$ 13 minutes.

Figure 1, shows an example of detected SB using PSP magnetic field data at 10s resolution. The z parameter is constantly above the selected threshold of 0.5 for $\sim$ 13 minutes. Notice that the reversal, using the definition Eq. 1 (as in Dudok de Wit et al. (2020)), is identified using the total magnetic field vector, and not only one component.

3. WAITING TIMES AND DURATION

The evaluation of the waiting time between two consecutive switchbacks and the duration of each event can provide insight to two fundamental questions: (I) do SBs tend to cluster, or are they more likely to be isolated events? (II) How do the waiting times and durations of switchbacks relate to turbulence scales, i.e., integral and inertial range scales? These questions address the issue of whether SBs are part of the evolving solar wind.

We define the duration of a SB as the number of consecutive above-threshold points times the cadence of magnetic field measurements employed (by this definition, a 1-point SB lasts 10s or 60s depending on the used dataset). In Fig. 1, the duration of ~ 13 minutes is given by all the consecutive above-threshold events comprised between the two vertical dashed lines. Instead, the waiting time (WT) between SBs is defined as the time elapsed between the end of a SB and the beginning of the following. This last measure is necessarily affected by the presence of missing data intervals. To avoid spurious too-long waiting times, we discard waiting times with values greater than $\mu + 3\sigma$ –where μ is the mean of all the WTs and σ is the standard deviation. Figure 2 shows the distribution of WTs and duration for the different settings used to analyze PSP and Wind data, along with a slope of reference.

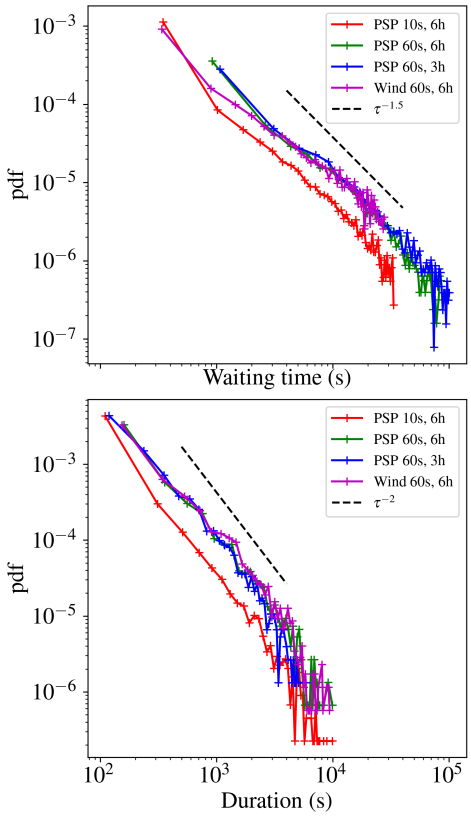

Figure 2. Distributions of (top) waiting times, and (bottom) SB duration, for the different tunable parameters – magnetic field time resolution and averaging window extension – used for PSP, and for Wind. Dashed lines are reference slopes.

Meaningful differences and similarities are evident in the distributions reported in Fig. 2. With respect to the magnetic field resolution, all those obtained with 60s magnetic field overlap quite well. As will be discussed below, the only difference appears in the Wind waiting time distribution. The act of modifying the averaging window between 3 or 6 hours does not produce any appreciable variation. Instead, using different magnetic field cadences appear to be associated with appreciable changes in the distribution of waiting times.

The distribution of SB duration shows a power law tail with a slope approaching -2. Therefore, an average duration can be estimated as $\langle \tau_{SB} \rangle = \int_0^\infty t \ \mathrm{pdf}(t) \ dt$, which varies between 200 and 500 seconds. Waiting time distributions, instead, show a slope closer to -1.5, for which the formal definition of an average WT is an ill-posed measure (Newman 2005). However, since the distributions have a finite extension, an approximate (population) average WT, ranging from 18 to 90 minutes, can be calculated with the available measurements.

Table 1 shows a summary of the above-mentioned results and parameters used for the analysis. Different columns list the spacecraft name, the magnetic field cadence, the width of the window, the average switchback duration, and the average switchback waiting time. The distribution of waiting times obtained with Wind measurements anticipates results to be discussed further in the next section. The maximum waiting time observed within all Wind measurements, is much lower than the average waiting time observed with PSP using the same cadence magnetic field (but also of the higher cadence). Therefore, we can infer that switchbacks are more common at 1 au since the average waiting time is shorter.

Consistent with previous discussions of switchbacks (Dudok de Wit et al. 2020) and discontinuities as measured by partial variance of increments (PVI) (Chhiber et al. 2020; Bandyopadhyay et al. 2020; Sioulas et al. 2022), we note that a powerlaw waiting time distribution is suggestive of *clustering*. That is, these distributions imply the presence of correlation between successive switchbacks.

SC	Δt (s)	W (h)	$\langle \tau_{SB} \rangle$ (s)	$\langle \tau_{WT} \rangle$ (s)	$\langle \tau_{WT} \rangle$ (min)
PSP	60	6	450	4000	66
PSP	60	3	370	5500	91
PSP	10	6	200	1100	18
Wind	60	6	503	2600	43

Table 1. Switchback average duration ($\langle \tau_{SB} \rangle$) and waiting times ($\langle \tau_{WT} \rangle$), evaluated over the period 2018 August 12 through 2021 June 19, by varying the spacecraft (SC), the magnetic field resolution (Δt), and the averaging window width (W).

4. RADIAL OCCURRENCE OF SWITCHBACKS

Early reports on switchbacks focused on PSP perihelia (Dudok de Wit et al. 2020; Mozer et al. 2020), and analyzed the first several orbits, with somewhat contrasting selection criteria, and correspondingly diverse results (Farrell et al. 2020; Mozer et al. 2021; Tenerani et al. 2021). With the release of the data from PSP orbit 8, the pool of available measurements spans about three years (1/3 of the total nominal mission duration), and the study of the radial evolution of switchbacks becomes more accessible and statistically relevant.

More recent studies (Liang et al. 2021; Martinović et al. 2021; Dudok de Wit et al. 2020) also report surveys, and vary rather significantly in both methodology and criteria for selecting events. To date, the origin of switchbacks remains a matter of debate.

Figure 3 shows a principal result of the present study – the joint distributions of the occurrence of magnetic switchbacks per 10^6 km vs PSP radial distance. The population in each bin is determined as follows: After having identified all the switchbacks as discussed in Sec. 2, we count how many SBs occur in one hour, and record the radial distance of PSP at that time. As one would expect, the occurrence of SBs would depend on the speed of the solar wind. If the spacecraft sits in a stream of slow wind, the chance to measure SBs per unit time are lower than those referring to a fast stream. To overcome this trivial dependence, we make use of the Taylor hypothesis (Jokipii 1973; Chhiber et al. 2019; Perez et al. 2021) to convert time intervals to spatial distances employing SWEAP and SWE hourly averaged measurements (for PSP and Wind respectively). Therefore, we obtain an occurrence rate per unit distance for each one hour sample, and focus on this quantity instead of the rate per unit time.

The rates are tabulated from all available data, and are sorted in the binned parameter space (R, ν) – where R is PSP radial distance and ν is the number of SBs per Mkm. When this has been accumulated over the entire population, we have obtained the joint distributions $J(R, \nu)$ that are shown in the color plots in panels (a, d) of Fig. 3. The color parameter is a measure of the logarithm of the probability density in a particular cell of the (R, ν) grid. An immediate impression is that a lower rate of SBs per km is is found at the smallest heliodistances.

A more direct view on the occurrence can be recovered via the marginal distributions that are obtained from the joint pdf. One marginal distribution is obtained by integration of the joint distribution over all radial distances, $J_\nu = \int J(R, \nu)\, dR$. This is the distribution of SB counts per Mkm without regard to the radial distance.

For the distribution computed from the 60s data, noting the strong peak in J_ν in the range of $1 < \nu < 2$, one draws a "trivial" interpretation that it is more common to find one or two SBs per Mkm than it is to find several. A more physical interpretation of this result becomes apparent when recalling that the mean value of correlation lengths in the solar wind in the inner heliosphere gradually increases from about 500,000 km to 1,000,000 km from 0.16 au to 1

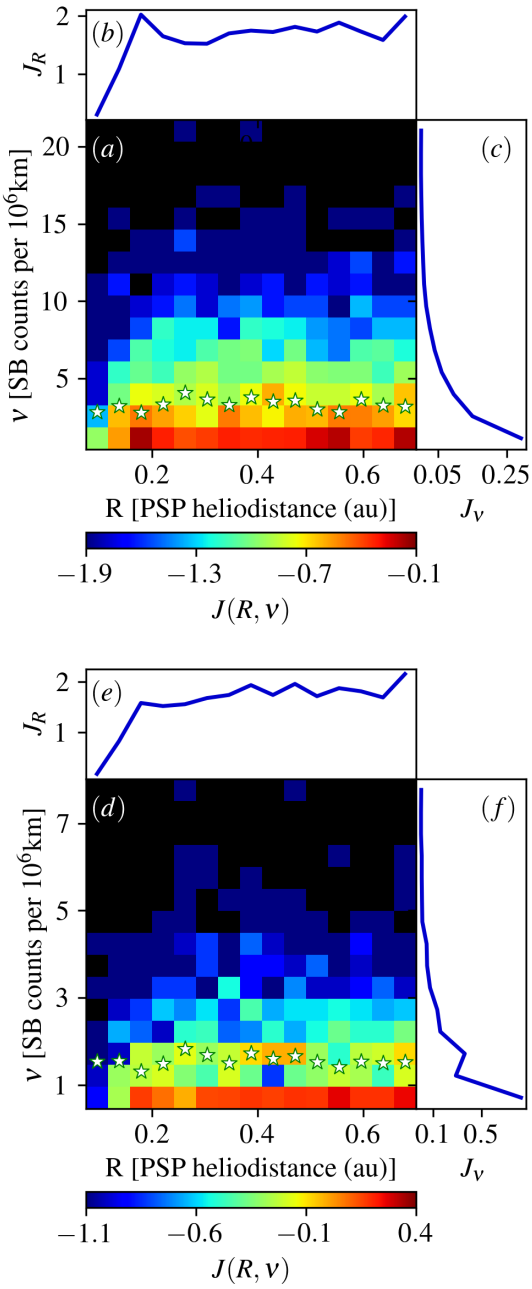

Figure 3. (Color plot) joint distribution $J(R,\nu)$ of SB counts per 10^6 km (ν) vs PSP heliodistance (R), using magnetic field at 10s (a) and 60s (d). Colors represent the probability distribution in log scale (black domains are regions with zero counts). The marginal probability distributions (see text) are shown in panels (b,c) for 10s and (e,f) for 60s magnetic field. White stars represent the average value $\langle\nu\rangle$ for each column, i.e. $\langle\nu\rangle = \frac{\int d\nu'\ \nu'\ F(\nu',R^*)}{\int d\nu'\ F(\nu',R^*)}$.

au (Ruiz et al. 2014; Chhiber et al. 2021; Cuesta et al. In prep.). Therefore, a simple interpretation of the substantial peaking of J_ν at values less than 2 for 60s magnetic field data, is that, averaged over the aggregate population within 1 au, switchbacks are found in the solar wind about once per correlation length. However, when 10s data is used in the calculation, the marginal distribution J_ν retains a similar shape, however stretched to a range of about $1 < \nu < 6$. This is consistent with the intuition that higher time resolution data can (and will) detect shorter time duration SBs that the coarser resolution data cannot detect.

The other interesting marginal distribution is $J_R = \int J(R,\nu)\, d\nu$, that is, the distribution of SBs per radial distance, as a function of the radial distance, and integrated over all possible local occurrence rates. This marginal distribution displays two distinct regimes: (I) descending below 0.2 au ($\sim 40\ R_\odot$) there is a sharp decrease in high SB count rates, and (II) a plateau is reached between $0.2 - 0.7$ au (The available data from PSP at distances beyond 0.7 au are insufficient).

As we did in Sec. 3, we replicate and compare the same analysis with Wind measurements at 1 au. Since Wind's position is approximately fixed, it is not possible to reproduce the full joint pdf; but, below, we will show that the average occurrence rates at Wind are compatible with the PSP observations.

The average number of switchbacks per Mkm, as a function of the heliodistance, can be obtained from the joint distributions in Fig. 3. Each column of the colour plot represents the distribution of the number of SBs per Mkm at a fixed heliodistance. From each of this conditioned distributions $F(\nu, R^*)$, it is possible to obtain the average ν for each fixed R^*, computing the normalized first moment $\int d\nu'\ \nu'\ F(\nu', R^*) / \int d\nu'\ F(\nu', R^*)$. Each column average value (or first moment) is displayed with a star-shaped symbol in Fig. 3. The same treatment holds for Wind, except only one value of R^* is present.

Again, we can notice that the first points (the four averages for $R \lesssim 0.25$ au) have values lower than the subsequent points, which seem to attain a plateau. An interesting physical interpretation arises if we consider the evolution of turbulence correlation length that can roughly be estimated as $\lambda_C \sim 10^6\ \mathrm{km}\sqrt{R(\mathrm{au})}$ (Ruiz et al. 2014; Cuesta et al. In prep.). After a simple transformation, we arrive at Fig. 4 which shows the average number of switchbacks per correlation length as a function of the radial distance. As a check, the same analysis has been performed by measuring the average number of switchback directly from the detected population, rather than using the moments of the conditioned distributions, and the results (not shown) are indistinguishable.

The novel organization of the mean values, in Fig. 4, points toward the following consideration: The average number of SBs per Mkm is constant, but the solar wind structure, in which they are embedded, is dynamically evolving. If we consider the correlation length to be the typical scale of turbulent eddies, the result that the average number of SBs per correlation length increases, somehow envisions that SBs can be also seen as a byproduct of turbulence and their presence is enhanced as the turbulent cascade takes place.

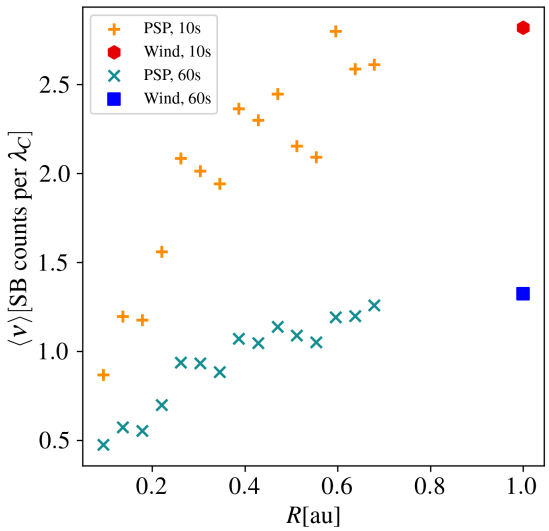

Figure 4. Average number of switchbacks per correlation length (estimated as $\lambda_C \sim 10^6\ \mathrm{km}\sqrt{R(\mathrm{au})}$), as a function of the heliodistance.

5. DISCUSSION OF THE RESULTS & CONCLUSION

The topic of switchbacks in PSP observations has become very active due to the dramatic nature of these observations and the possible implications that these large magnetic-field deflections may have for unraveling the physics of solar wind heating and acceleration (Bale et al. 2019; Kasper et al. 2019), which are central goals of the PSP mission.

Switchback observations, particularly the radial variations of their occurrence and other properties studied by PSP, may be relevant to revealing the basic physics of the nascent solar wind.

The prolific appearance of switchbacks in PSP datasets has prompted investigators to analyze *ensembles* of identified cases to establish statistical properties, and therefore, in principle, a robust physical perspective. These studies have adopted varying definitions, leading to disparate identification criteria, thus emphasizing different physical properties. For example, the defining conditions in some studies do not require local polarity reversals, but only angular deflections (Dudok de Wit et al. 2020). Other studies imply that high Alfvénicity should be a defining condition (Borovsky 2016; Horbury et al. 2018). Another approach is to identify source regions as a factor in the selection criteria (Tenerani et al. 2021). The approach employed here is intentionally simplified: we employ only the reversal of direction relative to a locally averaged field to be the sole fundamental condition for identifying a switchback. As an a posteriori check, we examined the fraction of our identified events to assess how many are likely to be associated with possible heliospheric current sheet crossings; the results indicate such current sheet crossings represent $\sim 2\%$ of the identified PSP events, and $\sim 0.3\%$ for the Wind events. Therefore, these cases do not have a substantial effect on the statistical descriptions we have provided.

There are of course subsidiary conditions that enter into the selection we have implemented. For example, as discussed in Section 2 the average magnetic field must be well-defined within the interval in question, and the appearance of too large a fraction of missing data points renders a particular time slice unusable. Our methodology, applied between 2018 August 12 and 2021 June 19, about 1042 days, yielded a total of 22,223 switchbacks using PSP 10 second data and 6 hour averaging interval. See Table 2 for a list including all configurations used in this study.

Δt(s)	W(h)	#SBs (PSP)	#SBs (Wind)
10	3	19141	23793
10	6	22223	29908
60	3	6458	8117
60	6	7556	9301

Table 2. Total number of switchbacks #SBs identified with PSP and Wind, varying the magnetic field cadence Δt in seconds and the averaging window width W in hours.

We note that we included analyses only of data at heliocentric distances $r < 0.7$ au, even though some data was available in the range 0.7 au $< r <$ 1 au. That range is excluded due to the relative scarcity of data. In part this is due to the PSP orbit aphelia, which barely extend beyond 0.7 au after orbit 6, as well as lower data availability in general in that range (Chhiber et al. 2021).

Characteristics of the observed switchback rates. A salient feature of the switchback occurrence rates seen in both Fig. 3 and Fig. 4 is the appearance of a ramp at $r < 0.25$ au (i.e., $\sim$48 $R_\odot$). A naive extrapolation of this trend to zero switchback rate occurs at around 20 solar radii. This is remarkably close to the radius at which the first passage into subAlfvénic coronal plasma was detected recently (Kasper et al. 2021; Chhiber et al. 2022). If one views this as an increase in switchback rate beginning at $\sim$ 20 solar radii, then the "turning on" of switchbacks in this range of heliocentric distances appears to support the hypothesis that shear driven activity is initiated in this vicinity. A proposed candidate is MHD mixing layer dynamics, leading to rollups of vorticity and magnetic field reversals (Ruffolo et al. 2020). This is also the same region in which the more striated coronal plasma transitions to a more isotropic *flocculated* appearance in heliospheric imaging analyses (DeForest et al. 2016; Chhiber et al. 2019) of the inner solar wind.

Beside the Ruffolo et al. (2020) model, there are other models for *in situ* generation of switchbacks (Squire et al. 2020; Schwadron & McComas 2021) that may also be consistent with the present observations. We also are not attempting here to garner evidence to controvert models for generation of switchbacks at much lower altitudes, such as interchange reconnection in the chromosphere or lower corona (Fisk & Kasper 2020; Drake, J. F. et al. 2021; Magyar et al. 2021a,b; Zank et al. 2020). In fact, there may be separate populations generated at lower altitudes that experience attenuation (Tenerani et al. 2020) during propagation to radii beyond the Alfvén transition zone, and a separate population that is initiated at higher altitudes (Tenerani et al. 2021).

It is noteworthy that transforming the data from a switchbacks per kilometer format to a switchbacks per correlation scale format, as in Figure 4, does appear to produce a systematic ordering of the data. For example, the trends at low heliocentric distance of switchbacks/λ_c for both magnetic cadences approach a zero count rate near 0.1 au.

Meanwhile, the relatively smooth increase at larger R extrapolates reasonably well to the Wind results at 1 au. It is tempting to interpret this as support for the idea that turbulence properties are, at some level, controlling or influencing switchback rates. However, it is difficult to assert that scaling to the correlation length is the only way to organize the data.

Albeit the driving of the source in the lower solar atmosphere is definitely responsible for defining some of the macroscopic features of turbulence (Bale et al. 2021; Fargette et al. 2021; Magyar et al. 2021a,b), given the systematic behavior of the switchback rate seen in Figure 4, there is a strong suggestion that switchback properties, including their rate of occurrence, are evolving and are controlled, at some level, by dynamics outside of about 0.1 au.

This research is partially supported by the Parker Solar Probe mission through the IS⊙IS Theory and Modeling team and a subcontract from Princeton University (SUB0000317), NASA PSP Guest Investigator grants 80NSSC21K1765 and 80NSSC21K1767, and NASA Heliospheric Supporting Research program grants 80NSSC18K1210 and 80NSSC18K1648. This project is also partially supported by the European Union's Horizon 2020 research and innovation program under grant agreement No. 776262 (AIDA, www.aida-space.eu). The PSP data used here is publicly available on NASA CDAWeb https://cdaweb.gsfc.nasa.gov/index.html/. The authors thank the FIELDS team (PI: Stuart D. Bale, UC Berkeley), the Integrated Science Investigation of the Sun (IS⊙IS) Science Team (PI: David McComas, Princeton University) and the Solar Wind Electrons, Alphas, and Protons (SWEAP) team for providing data (PI: Justin Kasper, BWX Technologies) for providing data. Parker Solar Probe was designed, built, and is now operated by the Johns Hopkins Applied Physics Laboratory as part of NASA's Living with a Star (LWS) program (contract NNN06AA01C). Support from the LWS management and technical team has played a critical role in the success of the Parker Solar Probe mission. FP thanks Mattia Rovito for his help with the design of the database webpage. LP thanks the ICT center of the University of Calabria for hosting the webserver of the database.

APPENDIX

A. ONLINE DATABASE OF DETECTED SWITCHBACKS

The present work afforded an opportunity to assemble an open-access online catalogue that accepts inquiries in the form of a specified time interval, and provides a list of magnetic field reversals and the time of their occurrence. Assembly of such a database requires analyzing a large amount of raw data (months or years), from the public PSP archive folders.

The reproduction of such data can be achieved by replicating the download and analysis steps; this sacrifices quickness in favor of economy of storage requirements. Another approach is to set up a capacious disk where storing all possibly needed data sets to access them rapidly using a simple interface. The assembled database supports the latter approach for convenience of the interested user.

The database is built using the parameters described in the paper. The user is asked to input the spacecraft (Wind or PSP), magnetic field cadence (10s or 60s), averaging window (3h or 6h), and a time interval (within the first 8 orbits of PSP). The output is immediately provided as a list of UTC seconds, human-readable dates, and the value of z, for all the points that satisfy $z \geq 0.5$. The user can then choose to print the output on screen, or download as a text file.

The database is freely accessible at http://astroplasmas.unical.it/SBDB/

REFERENCES

Bale, S. D., Goetz, K., Harvey, P. R., et al. 2016, Space Science Reviews, 204, 49, doi: 10.1007/s11214-016-0244-5

Bale, S. D., Badman, S. T., Bonnell, J. W., et al. 2019, Nature, 576, 237, doi: 10.1038/s41586-019-1818-7

Bale, S. D., Horbury, T. S., Velli, M., et al. 2021, The Astrophysical Journal, 923, 174, doi: 10.3847/1538-4357/ac2d8c

Bandyopadhyay, R., Matthaeus, W. H., Parashar, T. N., et al. 2020, The Astrophysical Journal Supplement Series, 246, 61, doi: 10.3847/1538-4365/ab6220

Bandyopadhyay, R., Matthaeus, W. H., McComas, D. J., et al. 2021, A&A, 650, L4, doi: 10.1051/0004-6361/202039800

Borovsky, J. E. 2016, Journal of Geophysical Research (Space Physics), 121, 5055, doi: 10.1002/2016JA022686

Chhiber, R., Matthaeus, W. H., Usmanov, A. V., Bandyopadhyay, R., & Goldstein, M. L. 2022, An Extended and Fragmented Alfvén Zone in the Young Solar Wind. https://arxiv.org/abs/2201.08422

Chhiber, R., Usmanov, A. V., Matthaeus, W. H., & Goldstein, M. L. 2019, Astrophys. J. Suppl., 241, 11, doi: 10.3847/1538-4365/ab0652

Chhiber, R., Usmanov, A. V., Matthaeus, W. H., & Goldstein, M. L. 2021, The Astrophysical Journal, 923, 89, doi: 10.3847/1538-4357/ac1ac7

Chhiber, R., Usmanov, A. V., Matthaeus, W. H., Parashar, T. N., & Goldstein, M. L. 2019, The Astrophysical Journal Supplement Series, 242, 12, doi: 10.3847/1538-4365/ab16d7

Chhiber, R., Goldstein, M. L., Maruca, B. A., et al. 2020, The Astrophysical Journal Supplement Series, 246, 31, doi: 10.3847/1538-4365/ab53d2

Cuesta, M. E., Chhiber, R., Roy, S., et al. In prep.

DeForest, C. E., Matthaeus, W. H., Viall, N. M., & Cranmer, S. R. 2016, Astrophys. J., 828, 66, doi: 10.3847/0004-637X/828/2/66

Drake, J. F., Agapitov, O., Swisdak, M., et al. 2021, A&A, 650, A2, doi: 10.1051/0004-6361/202039432

Dudok de Wit, T., Krasnoselskikh, V. V., Bale, S. D., et al. 2020, ApJS, 246, 39, doi: 10.3847/1538-4365/ab5853

Fargette, N., Lavraud, B., Rouillard, A. P., et al. 2021, The Astrophysical Journal, 919, 96, doi: 10.3847/1538-4357/ac1112

Farrell, W. M., MacDowall, R. J., Gruesbeck, J. R., Bale, S. D., & Kasper, J. C. 2020, The Astrophysical Journal Supplement Series, 249, 28, doi: 10.3847/1538-4365/ab9eba

Fisk, L. A., & Kasper, J. C. 2020, ApJL, 894, L4, doi: 10.3847/2041-8213/ab8acd

Fox, N. J., Velli, M. C., Bale, S. D., et al. 2016, Space Science Reviews, 204, 7, doi: 10.1007/s11214-015-0211-6

Horbury, T. S., Matteini, L., & Stansby, D. 2018, MNRAS, 478, 1980, doi: 10.1093/mnras/sty953

Horbury, T. S., Woolley, T., Laker, R., et al. 2020, ApJS, 246, 45, doi: 10.3847/1538-4365/ab5b15

Jokipii, J. R. 1973, Annual Review of Astronomy and Astrophysics, 11, 1, doi: 10.1146/annurev.aa.11.090173.000245

Kasper, J. C., Abiad, R., Austin, G., et al. 2016, Space Science Reviews, 204, 131, doi: 10.1007/s11214-015-0206-3

Kasper, J. C., Bale, S. D., Belcher, J. W., et al. 2019, Nature, 576, 228, doi: 10.1038/s41586-019-1813-z

Kasper, J. C., Klein, K. G., Lichko, E., et al. 2021, Phys. Rev. Lett., 127, 255101, doi: 10.1103/PhysRevLett.127.255101

Laker, R., Horbury, T. S., Bale, S. D., et al. 2021, A&A, 650, A1, doi: 10.1051/0004-6361/202039354

Landi, S., Hellinger, P., & Velli, M. 2006, Geophys. Res. Lett., 33, L14101, doi: 10.1029/2006GL026308

Lepping, R. P., Acũna, M. H., Burlaga, L. F., et al. 1995, SSRv, 71, 207, doi: 10.1007/BF00751330

Liang, H., Zank, G. P., Nakanotani, M., & Zhao, L.-L. 2021, The Astrophysical Journal, 917, 110, doi: 10.3847/1538-4357/ac0a73

Magyar, N., Utz, D., Erdélyi, R., & Nakariakov, V. M. 2021a, The Astrophysical Journal, 911, 75, doi: 10.3847/1538-4357/abec49

—. 2021b, The Astrophysical Journal, 914, 8, doi: 10.3847/1538-4357/abfa98

Martinović, M. M., Klein, K. G., Huang, J., et al. 2021, The Astrophysical Journal, 912, 28, doi: 10.3847/1538-4357/abebe5

McCracken, K., & Ness, N. 1966, Journal of Geophysical Research, 71, 3315

McManus, M. D., Bowen, T. A., Mallet, A., et al. 2020, ApJS, 246, 67, doi: 10.3847/1538-4365/ab6dce

Mozer, F. S., Bale, S. D., Bonnell, J. W., et al. 2021, The Astrophysical Journal, 919, 60, doi: 10.3847/1538-4357/ac110d

Mozer, F. S., Agapitov, O. V., Bale, S. D., et al. 2020, ApJS, 246, 68, doi: 10.3847/1538-4365/ab7196

Neugebauer, M., & Goldstein, B. E. 2013, AIP Conference Proceedings, 1539, 46, doi: 10.1063/1.4810986

Newman, M. 2005, Contemporary Physics, 46, 323, doi: 10.1080/00107510500052444

Ogilvie, K. W., Chornay, D. J., Fritzenreiter, R. J., et al. 1995, SSRv, 71, 55, doi: 10.1007/BF00751326

Perez, J. C., Bourouaine, S., Chen, C. H. K., & Raouafi, N. E. 2021, A&A, 650, A22, doi: 10.1051/0004-6361/202039879

Ruffolo, D., Matthaeus, W. H., Chhiber, R., et al. 2020, The Astrophysical Journal, 902, 94, doi: 10.3847/1538-4357/abb594

Ruiz, M. E., Dasso, S., Matthaeus, W. H., & Weygand, J. M. 2014, Solar Phys., 289, 3917, doi: 10.1007/s11207-014-0531-9

Schwadron, N., & McComas, D. 2021, The Astrophysical Journal, 909, 95

Sioulas, N., Velli, M., Chhiber, R., et al. 2022. https://arxiv.org/abs/2201.10067

Squire, J., Chandran, B. D. G., & Meyrand, R. 2020, ApJL, 891, L2, doi: 10.3847/2041-8213/ab74e1

Tenerani, A., Sioulas, N., Matteini, L., et al. 2021, The Astrophysical Journal Letters, 919, L31, doi: 10.3847/2041-8213/ac2606

Tenerani, A., Velli, M., Matteini, L., et al. 2020, Astrophys. J. Suppl., 246, 32, doi: 10.3847/1538-4365/ab53e1

Zank, G. P., Nakanotani, M., Zhao, L.-L., Adhikari, L., & Kasper, J. 2020, The Astrophysical Journal, 903, 1, doi: 10.3847/1538-4357/abb828